J|A|C|S
ARTICLES
Published on Web 02/02/2007

Probing Hydrogen Bonding and Ion−Carbonyl Interactions by Solid-State ^{17}O NMR Spectroscopy: G-Ribbon and G-Quartet

Irene C. M. Kwan, Xin Mo, and Gang Wu*

Contribution from the Department of Chemistry, Queen's University, 90 Bader Lane, Kingston, Ontario, Canada K7L 3N6

Received November 10, 2006; E-mail: gangwu@chem.queensu.ca

Abstract: We report solid-state ^{17}O NMR determination of the ^{17}O NMR tensors for the keto carbonyl oxygen (O6) of guanine in two ^{17}O-enriched guanosine derivatives: [6-^{17}O]guanosine (**G1**) and 2′,3′,5′-*O*-triacetyl-[6-^{17}O]guanosine (**G2**). In **G1**·$2H_2O$, guanosine molecules form hydrogen-bonded G-ribbons where the guanine bases are linked by O6···H−N2 and N7···H−N7 hydrogen bonds in a zigzag fashion. In addition, the keto carbonyl oxygen O6 is also weakly hydrogen-bonded to two water molecules of hydration. The experimental ^{17}O NMR tensors determined for the two independent molecules in the asymmetric unit of **G1**·$2H_2O$ are: Molecule A, $C_Q = 7.8 \pm 0.1$ MHz, $\eta_Q = 0.45 \pm 0.05$, $\delta_{iso} = 263 \pm 2$, $\delta_{11} = 460 \pm 5$, $\delta_{22} = 360 \pm 5$, $\delta_{33} = -30 \pm 5$ ppm; Molecule B, $C_Q = 7.7 \pm 0.1$ MHz, $\eta_Q = 0.55 \pm 0.05$, $\delta_{iso} = 250 \pm 2$, $\delta_{11} = 440 \pm 5$, $\delta_{22} = 340 \pm 5$, $\delta_{33} = -30 \pm 5$ ppm. In **G1**/K^+ gel, guanosine molecules form extensively stacking G-quartets. In each G-quartet, four guanine bases are linked together by four pairs of O6···H−N1 and N7···H−N2 hydrogen bonds in a cyclic fashion. In addition, each O6 atom is simultaneously coordinated to two K^+ ions. For **G1**/K^+ gel, the experimental ^{17}O NMR tensors are: $C_Q = 7.2 \pm 0.1$ MHz, $\eta_Q = 0.68 \pm 0.05$, $\delta_{iso} = 232 \pm 2$, $\delta_{11} = 400 \pm 5$, $\delta_{22} = 300 \pm 5$, $\delta_{33} = -20 \pm 5$ ppm. In the presence of divalent cations such as Sr^{2+}, Ba^{2+}, and Pb^{2+}, **G2** molecules form discrete octamers containing two stacking G-quartets and a central metal ion, that is, $(\mathbf{G2})_4-M^{2+}-(\mathbf{G2})_4$. In this case, each O6 atom of the G-quartet is coordinated to only one metal ion. For **G2**/M^{2+} octamers, the experimental ^{17}O NMR parameters are: Sr^{2+}, $C_Q = 6.8 \pm 0.1$ MHz, $\eta_Q = 1.00 \pm 0.05$, $\delta_{iso} = 232 \pm 2$ ppm; Ba^{2+}, $C_Q = 7.0 \pm 0.1$ MHz, $\eta_Q = 0.68 \pm 0.05$, $\delta_{iso} = 232 \pm 2$ ppm; Pb^{2+}, $C_Q = 7.2 \pm 0.1$ MHz, $\eta_Q = 1.00 \pm 0.05$, $\delta_{iso} = 232 \pm 2$ ppm. We also perform extensive quantum chemical calculations for the ^{17}O NMR tensors in both G-ribbons and G-quartets. Our results demonstrate that the ^{17}O chemical shift tensor and quadrupole coupling tensor are very sensitive to the presence of hydrogen bonding and ion−carbonyl interactions. Furthermore, the effect from ion−carbonyl interactions is several times stronger than that from hydrogen-bonding interactions. Our results establish a basis for using solid-state ^{17}O NMR as a probe in the study of ion binding in G-quadruplex DNA and ion channel proteins.

1. Introduction

Oxygen is one of the most common elements found in organic and biological molecules. Oxygen atoms are often involved in two major types of intermolecular interactions: hydrogen bonding and ion−ligand interactions. These interactions can be found in almost all biomolecular structures and play crucial roles in biological processes. Among oxygen-containing functional groups, carbonyl oxygen (C═O) is perhaps the most important one, because carbonyl oxygen atoms are ubiquitous in proteins (backbone and side chains) and nucleic acid bases. The hydrogen-bonding interaction between carbonyl oxygen atoms (C═O) and other functional groups such as N−H and O−H plays a major role in the formation and stability of high-order structures formed from these biological molecules.[1] In addition to hydrogen bonding, metal ion−carbonyl interactions are also important in many biological structures. For example, carbonyl oxygen atoms are often involved in the catalytic sites of metalloenzymes. Another important class of proteins of biological significance is ion channel proteins. The recent crystal structure of K^+ ion channel protein, KcsA,[2−5] provides a remarkable example illustrating structural details about ion−carbonyl interactions and how the ion−carbonyl interaction plays a key role in ion selectivity. Traditionally, ^{13}C and ^{15}N NMR techniques are used to probe ion−carbonyl interactions in ion channels;[6−8] however, ^{17}O NMR should be more sensitive to ion−carbonyl interactions than ^{13}C and ^{15}N NMR for the following three reasons. First, the oxygen atom of a carbonyl group is directly involved in the ion−carbonyl interaction. Second, the chemical shift range for ^{17}O is several times larger

(1) Jeffrey, G. A.; Saenger, W. *Hydrogen Bonding in Biological Structures*; Springer-Verlag: Berlin, 1991.
(2) Doyle, D. A.; Cabral, J. M.; Pfuetzner, R. A.; Kuo, A. L.; Gulbis, J. M.; Cohen, S. L.; Chait, B. T.; MacKinnon, R. *Science* **1998**, *280*, 69.
(3) Morais-Cabral, J. H.; Zhou, Y.; MacKinnon, R. *Nature* **2001**, *414*, 37.
(4) Zhou, Y. F.; Morais-Cabral, J. H.; Kaufman, A.; MacKinnon, R. *Nature* **2001**, *414*, 43.
(5) MacKinnon, R. *Angew. Chem., Int. Ed.* **2004**, *43*, 4265.
(6) Smith, R.; Thomas, D. E.; Atkins, A. R.; Separovic, F.; Cornell, B. A. *Biochim. Biophys. Acta* **1990**, *1026*, 161.
(7) Tian, F.; Lee, K.-C.; Hu, W.; Cross, T. A. *Biochemistry* **1996**, *35*, 11959.
(8) Tian, F.; Cross, T. A. *J. Magn. Reson.* **1998**, *135*, 535.

10.1021/ja067991m CCC: $37.00

than those for ^{13}C and ^{15}N. Third, because ^{17}O is a quadrupolar nucleus, the quadrupole coupling tensor often provides additional information about the chemical bonding. Of course, the major challenge is to overcome the practical difficulties associated with solid-state NMR experiments for quadrupolar nuclei such as ^{17}O compared with spin-1/2 nuclei such as ^{13}C and ^{15}N.

In the past several years, we and others have accumulated a considerable amount of information about the effects of hydrogen bonding on ^{17}O NMR tensors (quadrupole coupling tensor and chemical shift tensor) in a variety of organic compounds.[9−25] In comparison, much less is known about the effect of ion−carbonyl interactions on ^{17}O NMR tensors. In a solid-state ^{17}O NMR study for potassium hydrogen dibenzoate (PHB), we noted that, to reliably reproduce the experimental ^{17}O NMR tensors by quantum chemical calculations, K^+−O interactions must be included in the molecular model.[18] In a recent experimental study, Hu et al.[26] demonstrated for the first time that high-quality ^{17}O NMR spectra can be obtained for both powdered and oriented gramicidin A samples (57% ^{17}O-labeled at Leu10) at a high magnetic field. More importantly, they showed that the ^{17}O NMR signal from ^{17}O-[D-Leu10]gA uniformly aligned in DMPC bilayers is remarkably sensitive to the presence of K^+ ions, suggesting that ^{17}O can be used as a new nuclear probe for characterizing ion−carbonyl interactions in ion channels. Subsequently, Chekmenev et al.[27] reported an in-depth examination of the effect of ion−carbonyl interactions on the ^{17}O NMR tensors for the carbonyl oxygen in a model peptide GlyGlyGly. They observed that both the ^{17}O isotropic chemical shift and quadrupole coupling constant are significantly reduced when the carbonyl oxygen atom is involved in ion−carbonyl interactions with Li^+ and Ca^{2+}. These observations further establish that the remarkable sensitivity of ^{17}O NMR tensors on ion−carbonyl interactions can potentially be used to study gating and selectivity in ion channels. Chekmenev et al.[28] also used solid-state ^{17}O NMR to demonstrate a reversible K^+ ion binding to gA pore. These recent studies appear to be the only examples in the literature to use solid-state ^{17}O NMR for probing ion−carbonyl interactions in organic and biological molecules. Here, we report on a solid-state ^{17}O NMR study of [6-^{17}O]guanosine derivatives; Scheme 1.

Scheme 1

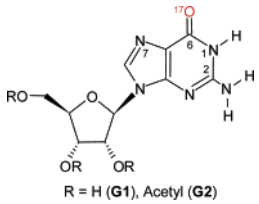

We chose guanosine derivatives because guanosine molecules are known to be able to form not only hydrogen-bonded molecular ribbons known as G-ribbons, but also a tetramer, known as the G-quartet, where four guanine bases are held together by eight hydrogen bonds.[29] The most important feature of the G-quartet structure is that it is usually stabilized by ion−carbonyl interactions between O6 and a variety of metal ions (Na^+, K^+, Rb^+, Sr^{2+}, Ba^{2+}, Pb^{2+}, etc.). In the past several years, we have developed a solid-state NMR approach to directly detect alkali metal ions such as $^{23}Na^+$, $^{39}K^+$, and $^{87}Rb^+$ in G-quartet systems including G-quadruplex DNA.[30−36] Recently, Brown and co-workers[37] also showed that solid-state ^{15}N NMR can be used to distinguish G-ribbons from G-quartets. Clearly, guanosine derivatives are also ideal molecular systems for solid-state ^{17}O NMR studies because the carbonyl oxygen atom O6 is at the center of action (i.e., directly involved in both hydrogen bonding and ion−carbonyl interactions). Another reason for our interest in the measurement of ^{17}O NMR tensors in G-quartets is due to the possibility that the channel structure formed by stacking G-quartets in G-quadruplex DNA may behave like an ion channel as first suggested by Hud et al.[38] Recent high-resolution crystal structures for both K^+ ion channels and G-quadruplex DNA oligomers have revealed a striking similarity in ion coordination between these two very different biomolecular systems. For example, in the selectivity filter of KcsA, each K^+ ion is coordinated to eight peptide carbonyl oxygen atoms in a square anti-prism fashion,[5] whereas in the cavity of the G-quadruplex formed by d($G_4T_4G_4$),[39] each K^+ ion is also coordinated to eight carbonyl oxygen atoms in a way almost identical to that seen in KcsA. Because of these structural similarities, we anticipate that any knowledge about ^{17}O NMR tensors in G-quartets may help establish the basis for using solid-state ^{17}O NMR as an effective probe in the study of ion binding in both G-quadruplex DNA and ion channel proteins.

Because ion−carbonyl interactions in G-quartets always coexist with hydrogen-bonding interactions, it is important to

(9) Kuroki, S.; Takahashi, A.; Ando, I.; Shoji, A.; Ozaki, T. *J. Mol. Struct.* **1994**, *323*, 197.
(10) Takahashi, A.; Kuroki, S.; Ando, I.; Ozaki, T.; Shoji, A. *J. Mol. Struct.* **1998**, *442*, 195.
(11) Wu, G.; Yamada, K.; Dong, S.; Grondey, H. *J. Am. Chem. Soc.* **2000**, *122*, 4215.
(12) Yamada, K.; Dong, S.; Wu, G. *J. Am. Chem. Soc.* **2000**, *122*, 11602.
(13) Dong, S.; Ida, R.; Wu, G. *J. Phys. Chem. A* **2000**, *104*, 11194.
(14) Wu, G.; Hook, A.; Dong, S.; Yamada, K. *J. Phys. Chem. A* **2000**, *104*, 4102.
(15) Wu, G.; Dong, S.; Ida, R. *Chem. Commun.* **2001**, 891.
(16) Wu, G.; Dong, S. *J. Am. Chem. Soc.* **2001**, *123*, 9119.
(17) Wu, G.; Dong, S.; Ida, R.; Reen, N. *J. Am. Chem. Soc.* **2002**, *124*, 1768.
(18) Wu, G.; Yamada, K. *Solid State Nucl. Magn. Reson.* **2003**, *24*, 196.
(19) Zhang, Q. W.; Chekmenev, E. Y.; Wittebort, R. J. *J. Am. Chem. Soc.* **2003**, *125*, 9140.
(20) Lemaitre, V.; Pike, K. J.; Watts, A.; Anupold, T.; Samoson, A.; Smith, M. E.; Dupree, R. *Chem. Phys. Lett.* **2003**, *371*, 91.
(21) Pike, K. J.; Lemaitre, V.; Kukol, A.; Anupold, T.; Samoson, A.; Howes, A. P.; Watts, A.; Smith, M. E.; Dupree, R. *J. Phys. Chem. B* **2004**, *108*, 9256.
(22) Yates, J. R.; Pickard, C. J.; Payne, M. C.; Dupree, R.; Profeta, M.; Mauri, F. *J. Phys. Chem. A* **2004**, *108*, 6032.
(23) Gervais, C.; Dupree, R.; Pike, K. J.; Bonhomme, C.; Profeta, M.; Pickard, C. J.; Mauri, F. *J. Phys. Chem. A* **2005**, *109*, 6960.
(24) Wong, A.; Pike, K. J.; Jenkins, R.; Clarkson, G. J.; Anupold, T.; Howes, A. P.; Crout, D. H. G.; Samoson, A.; Dupree, R.; Smith, M. E. *J. Phys. Chem. A* **2006**, *110*, 1824.
(25) Waddell, K. W.; Chekmenev, E. Y.; Wittebort, R. J. *J. Phys. Chem. B* **2006**, *110*, 22935.
(26) Hu, J.; Chekmenev, E. Y.; Gan, Z.; Gor'kov, P. L.; Saha, S.; Brey, W. W.; Cross, T. A. *J. Am. Chem. Soc.* **2005**, *127*, 11922.
(27) Chekmenev, E. Y.; Waddell, K. W.; Hu, J.; Gan, Z.; Wittebort, R. J.; Cross, T. A. *J. Am. Chem. Soc.* **2006**, *128*, 9849.
(28) Chekmenev, E. Y.; Gor'kov, P. L.; Cross, T. A.; Alaouie, A. M.; Smirnov, A. I. *Biophys. J.* **2006**, *91*, 3076.
(29) Davis, J. T. *Angew. Chem., Int. Ed.* **2004**, *43*, 668.
(30) Wu, G.; Wong, A. *Chem. Commun.* **2001**, 2658.
(31) Wong, A.; Fettinger, J. C.; Forman, S. L.; Davis, J. T.; Wu, G. *J. Am. Chem. Soc.* **2002**, *124*, 742.
(32) Wong, A.; Wu, G. *J. Am. Chem. Soc.* **2003**, *125*, 13895.
(33) Wu, G.; Wong, A.; Gan, Z. H.; Davis, J. T. *J. Am. Chem. Soc.* **2003**, *125*, 7182.
(34) Wu, G.; Wong, A. *Biochem. Biophys. Res. Commun.* **2004**, *323*, 1139.
(35) Ida, R.; Wu, G. *Chem. Commun.* **2005**, 4294.
(36) Wu, G.; Wong, A. Solid-state nuclear magnetic resonance studies of alkali metal ions in nucleic acids and related systems. In *NMR Spectroscopy of Biological Solids*; Ramamoorthy, A., Ed.; CRC Press: Boca Raton, FL, 2006; p 317.
(37) Pham, T. N.; Masiero, S.; Gottarelli, G.; Brown, S. P. *J. Am. Chem. Soc.* **2005**, *127*, 16018.
(38) Hud, N. V.; Smith, F. W.; Anet, F. A. L.; Feigon, J. *Biochemistry* **1996**, *35*, 15383.
(39) Haider, S.; Parkinson, G. N.; Neidle, S. *J. Mol. Biol.* **2002**, *320*, 189.

Scheme 2. Different Modes of Hydrogen Bonding for Guanosine Derivatives

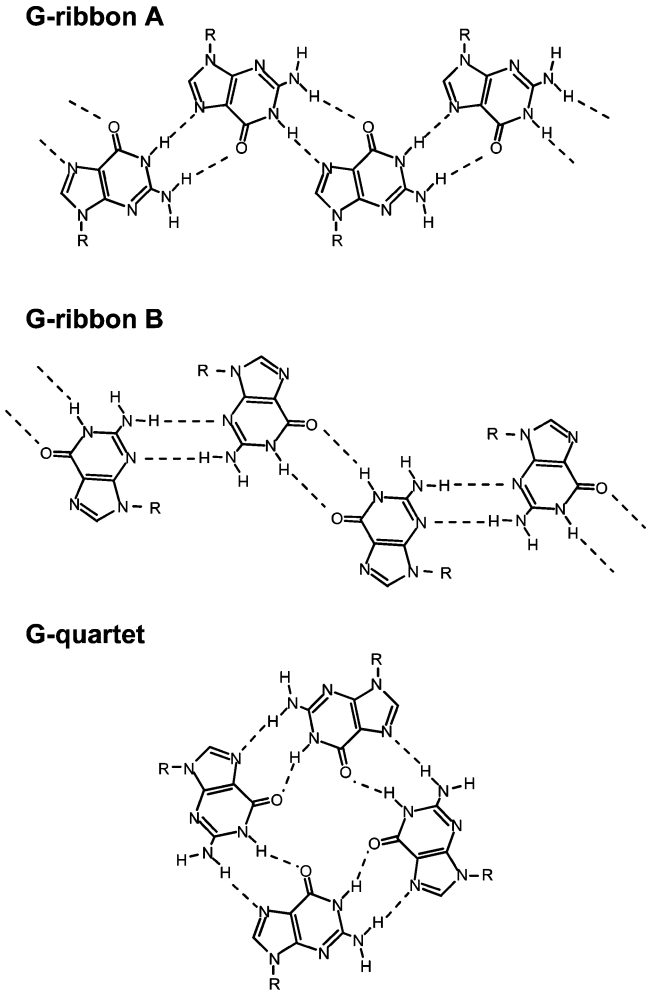

examine these two interactions separately. For guanosine derivatives, several possible types of hydrogen-bonding networks exist. As illustrated in Scheme 2, guanosine molecules can form either a G-ribbon or G-quartet. For the G-ribbon structure, there are also two different arrangements: G-ribbon A and G-ribbon B. For G-ribbon A, guanosine molecules are linked by O6···H−N2 and N7···H−N1 hydrogen bonds in a zigzag fashion, whereas in G-ribbon B, two different hydrogen bonds are observed: O6···H−N1 and N3···H−N2. In G-ribbon A, molecules are related by a crystallographic 2_1 symmetry so that each G-ribbon has a net nonzero dipole moment. In contrast, molecules in G-ribbon A are related by a center of inversion symmetry, which results in a vanishing dipole moment for the entire G-ribbon. G-ribbon A has been observed in many crystal structures ranging from guanine monohydrate[40] to guanosine nucleosides;[41−44] in contrast, G-ribbon B has only been observed to exist in organic solvents.[44] In G-quartet structures, the carbonyl oxygen O6 atom is not only involved in direct hydrogen bonding, but also coordinated to metal ions, M^{n+}

Scheme 3. Different Modes of Ion Binding in G-Quartets

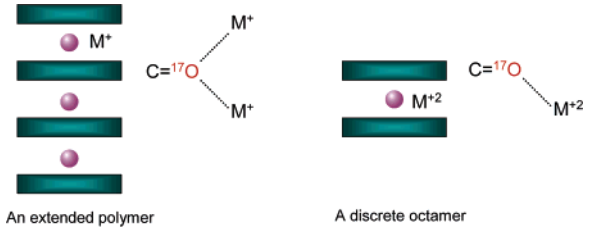

($n = 1, 2$). As illustrated in Scheme 3, with a monovalent cation, the G-quadruplex structure often consists of an extensive array of stacking G-quartets. With a divalent cation, on the other hand, discrete octamers are usually formed with a central cation, because the strong repulsion between two divalent cations prevents two octamers from stacking on top of each other. It should be noted that stacking of two G_8/M^{2+} octamers is possible in the presence of some "linking" ligands, as demonstrated by Davis and co-workers.[45] Consequently, depending on the nature of metal ions involved, there exist two different modes of ion−carbonyl interaction from the carbonyl oxygen point of view. As also illustrated in Scheme 3, with monovalent cations (alkali metals, NH_4^+ and Tl^+), each O6 is simultaneously coordinated to two cations with a typical M^+−O6 distance of 2.80 Å, whereas with divalent cations (Sr^{2+}, Ba^{2+}, Pb^{2+}), each O6 is coordinated to only one cation with a typical M^{2+}−O6 distance of 2.66 Å.

The objective of this study is to experimentally determine the ^{17}O NMR tensors in both G-ribbons and G-quartets at two magnetic fields, 11.75 and 21.15 T. G-ribbons are used to examine the hydrogen-bonding effect on ^{17}O NMR tensors, and G-quartets are used to evaluate the influence from ion−carbonyl interactions. We also perform extensive quantum chemical calculations for ^{17}O NMR tensors to aid separation of these different effects.

2. Experimental Section

Sample Preparation. All common chemicals and solvents were purchased from Sigma-Aldrich (Oakville, Ontario). Water (10% ^{17}O atom) was purchased from Cambridge Isotope Laboratories, Inc. (Andover, MA). Detailed descriptions for sample syntheses are given below.

[6-^{17}O]Guanosine. [6-^{17}O]Guanosine was prepared by an enzymatic reaction following a literature procedure.[46] To 10.1 units of adenosine deaminase (E.C. 3.5.4.4, crude powder obtained from Sigma-Aldrich, Lot No. 070H8145) was added 2.85 mL of 0.1 M sodium phosphate buffer (pH 7.0) prepared with ^{17}O-labeled water (10% ^{17}O atom) and 31.45 mg of 2-amino-6-chloropurine riboside (33 mM) dissolved in 0.15 mL of DMSO. The solution was incubated at 37 °C for 20 h. Over this period of time, white precipitates were produced in solution, which were then collected by centrifugation at 4000 rpm for 10 min. The white precipitates ([6-^{17}O]guanosine) were washed with cold water (3 × 1 mL) and then dried under N_2. Yield: 21 mg, 70%. Each batch of enzyme can be used three times before the activity of the enzyme notably decreases. The purity of the compound was verified by ^1H, ^{13}C, and ^{17}O NMR spectra. The solid product was [6-^{17}O]gaunosine dihydrate as confirmed by X-ray powder diffraction (XRD).

2′,3′,5′-*O*-Triacetyl-[6-^{17}O]guanosine. [6-^{17}O]Guanosine (142 mg, 0.5 mmol) was suspended in a mixture of CH_3CN (5 mL), dried pyridine (0.5 mL), and acetic anhydride (0.47 mL, 0.5 mmol). The mixture was

(40) Thewalt, U.; Bugg, C. E.; Marsh, R. E. *Acta Crystallogr.* **1971**, *B27*, 2358.
(41) Thewalt, U.; Bugg, C. E.; Marsh, R. E. *Acta Crystallogr.* **1970**, *B26*, 1089.
(42) Wilson, C. C.; Low, J. N.; Tollin, P. *Acta Crystallogr.* **1985**, *C41*, 1123.
(43) Low, J. N.; Tollin, P.; Wilson, C. C.; Scrimgeour, S. N. *Acta Crystallogr.* **1986**, *C42*, 700.
(44) Giorgi, T.; Grepioni, F.; Manet, I.; Mariani, P.; Masiero, S.; Mezzina, E.; Pieraccini, S.; Saturni, L.; Spada, G. P.; Gottarelli, G. *Chem.−Eur. J.* **2002**, *8*, 2143.
(45) Shi, X. D.; Mullaugh, K. M.; Fettinger, J. C.; Jiang, Y.; Hofstadler, S. A.; Davis, J. T. *J. Am. Chem. Soc.* **2003**, *125*, 10830.
(46) Rayat, S.; Majumdar, P.; Tipton, P.; Glaser, R. *J. Am. Chem. Soc.* **2004**, *126*, 9960.

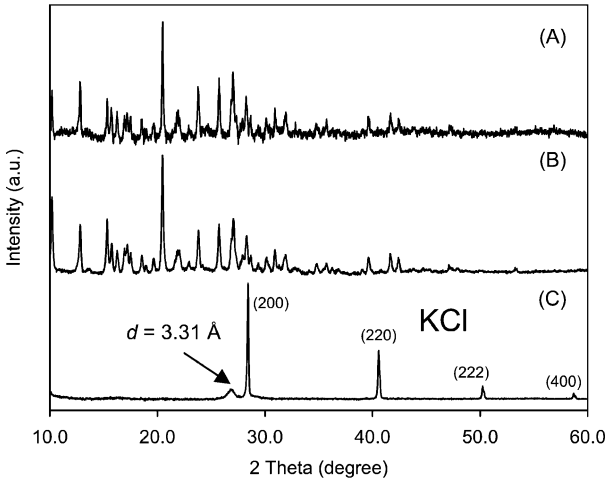

Figure 1. Powder XRD spectra obtained for (A) commercial guanosine·$2H_2O$, (B) [6-^{17}O]guanosine·$2H_2O$, and (C) [6-^{17}O]guanosine/K^+ gel. The peak at $d = 3.31$ Å confirms the formation of stacking G-quartets in (C).

stirred for 3 h at room temperature until the reaction was completed as indicated by TLC analysis. The solvent was removed under reduced pressure, and the organic phase was washed with water (3 × 3 mL). The residue was suspended in 2 mL of water and lyophilized to give white powders of 2′,3′,5′-*O*-triacetyl-[6-^{17}O]guanosine. Yield: 151 mg, 75%. The purity of the compound was verified by ^{1}H, ^{13}C, and ^{17}O NMR spectra.

[6-^{17}O]Guanosine-K^+ Gel. To 0.6 mL of 0.1 M KCl(aq) was added 15.29 mg of [6-^{17}O]guanosine. The suspension solution was heated at 90 °C until all contents were dissolved. A transparent gel was formed upon cooling of the hot solution to room temperature. The observed hydrogel was an indication of the formation of high-order self-assembly based on the G-quartet. The gel was then dried under N_2 and used directly in solid-state NMR and powder XRD analyses.

2′,3′,5′-*O*-Triacetyl-[6-^{17}O]guanosine/M^{+2} Octamers. Complexes of Sr^{+2} and Ba^{+2} picrates with 2′,3′,5′-*O*-triacetyl-[6-^{17}O]guanosine were prepared following a liquid−liquid extraction procedure established by Davis and co-workers.[47] To prepare the Pb^{+2} complex, we used only $PbCl_2$(aq) as the source of Pb^{+2}. In each case, the formation of G_8/M^{+2} complexes in $CDCl_3$ was confirmed by ^{1}H NOESY spectra; see Supporting Information. Powders were obtained after evaporation of $CDCl_3$ and were used in the solid-state NMR experiments.

X-ray Powder Diffraction Experiments. All XRD spectra were obtained on a Philips X'Pert Pro Multi Purpose diffractometer, using Ni-filtered Cu Kα 1, 2 radiation ($\lambda_1 = 1.5406$ Å, $\lambda_2 = 1.5444$ Å), with a fixed divergence slit width of 0.5° and 0.02 rad soller slit with 15-mm mask. The data were collected from 10 to 70° using X'pert X'celerator detector. Samples were loaded onto flat borosilicate discs and were rotated at 2 s per revolution. Data were processed on a Pentium PC, using PanAlytical X'pert HighScore for the Window XP.

Solid-State ^{17}O NMR. Solid-state ^{17}O NMR spectra at 11.75 T were recorded on a Bruker Avance-500 NMR spectrometer operating at 67.78 MHz for ^{17}O nuclei. A 4-mm MAS probe was used in both MAS and static experiments. A Hahn-echo sequence[48] was employed to record both MAS and static ^{17}O NMR spectra. The effective 90 and 180° pulse widths for the ^{17}O central transition were 1.0 and 2.0 μs, respectively. To record the MAS spectra, the interpulse delay was synchronized with the sample spinning period. Solid-state ^{17}O NMR spectra at 21.15 T were recorded on a Bruker Avance-II spectrometer operating at 122.08 MHz for ^{17}O nuclei. A 3.2-mm HX MAS probe was used with 70 kHz ^{1}H decoupling. Typically, a sample spinning frequency of 18 kHz was used in the MAS experiment. Other experimental details are given in figure captions.

Quantum Mechanical Calculations. All quantum mechanical calculations were performed using Gaussian03 software package[49] on Sun Fire 25000 servers configured with 72 × dual-core UltraSPARC-IV+1.5 GHz processors with 576 GB of RAM. SHELXTL[50] was used to construct molecular cluster models. Positions of hydrogen atoms, if not reported in the crystallographic studies, were calculated using standard bond distances. All quantum chemical calculations were performed at the density functional theory (DFT) level using the hybrid B3LYP exchange functional. The principal components of the electric field gradient tensor, q_{ii} ($ii = xx, yy, zz$; $|q_{zz}| > |q_{yy}| > |q_{xx}|$ and $q_{zz} + q_{yy} + q_{xx} = 0$), were computed in atomic units (1 au = 9.717365 × 10^{21} V m^{-2}). The principal magnetic shielding tensor components (σ_{ii}) were computed with $\sigma_{iso} = (\sigma_{11} + \sigma_{22} + \sigma_{33})/3$ and $\sigma_{33} > \sigma_{22} > \sigma_{11}$. In solid-state NMR experiments for quadrupolar nuclei, the measurable quantities for a quadrupole coupling tensor are quadrupole coupling constant (C_Q) and asymmetry parameter (η_Q). To compare calculated results with experimental NMR parameters, the following equations were used:

$$C_Q[\text{MHz}] = e^2 q_{zz} Q/h = -243.96 \times Q[\text{barn}] \times q_{zz}[\text{au}] \quad (1)$$

$$\eta_Q = (q_{xx} - q_{yy})/q_{zz} \quad (2)$$

where Q is the nuclear quadrupole moment, e is the elementary charge, and h is the Planck constant. The standard value for $Q(^{17}O)$, 2.558 × 10^{-28} m^2, was used in our study.[51]

The gauge including atomic orbital approach was used in chemical shielding calculations. To make a direct comparison between the calculated chemical shielding, σ, and the observed chemical shift, δ, we used the new absolute ^{17}O chemical shielding scale established by Wasylishen and Bryce:[52]

$$\delta\ (\text{ppm}) = 287.5\ (\text{ppm}) - \sigma\ (\text{ppm}) \quad (3)$$

In the quantum chemical calculations, we used correlation-consistent basis sets, cc-pVTZ, for all nonmetal atoms, except in the $(\mathbf{G2})_8/M^{2+}$ octamers where cc-pVTZ and 6-31G(d) were used for the target O6 atom and other nonmetal atoms, respectively. For alkali metal atoms, we used triple-ζ split valence basis sets of 6-311G for Na and K and the all-electron pVTZ basis set of Sadlej[53] for Rb. For Sr, Ba, and Pb atoms, we used the CRENBL basis sets,[54] which include a large orbital basis and a relativistic effective core potential for a small core (core electrons: Sr, 28; Ba, 46; Pb, 68). These basis sets were obtained from the Basis Set Exchange (http://gnode2.pnl.gov/bse/portal), which was developed by the Collaboratory for Multi-Scale Chemical Science in cooperation with the Environmental Molecular Sciences Laboratory (EMSL) and operated and maintained by EMSL, Pacific Northwest National Laboratory.

3. Results and Discussion

X-ray Powder Diffraction. Before we present solid-state ^{17}O NMR data, it is necessary to confirm the nature of the guanosine samples prepared for solid-state NMR experiments. In addition, because the crystal structure of guanosine dihydrate was used to construct a model for computations of ^{17}O NMR tensors, it was necessary to verify the crystal form of the NMR samples.

(47) Forman, S. L.; Fettinger, J. C.; Pieraccini, S.; Gottareli, G.; Davis, J. T. *J. Am. Chem. Soc.* **2000**, *122*, 4060.
(48) Kunwar, A. C.; Turner, G. L.; Oldfield, E. *J. Magn. Reson.* **1986**, *69*, 124.
(49) Frisch, M. J.; et al. *Gaussian 03*, revision C.02; Gaussian, Inc.: Wallingford, CT, 2004.
(50) *SHELXTL Crystal Structure Analysis Package*, version 5; Bruker Analytical X-ray System, Siemens: Madison, WI, 1995.
(51) Pyykko, P. *Mol. Phys.* **2001**, *99*, 1617.
(52) Wasylishen, R. E.; Bryce, D. L. *J. Chem. Phys.* **2002**, *117*, 10061.
(53) Sadlej, A. J. *Theor. Chim. Acta* **1992**, *81*, 45.
(54) LaJohn, L. A.; Christiansen, P. A.; Ross, R. B.; Atashroo, T.; Ermler, W. C. *J. Chem. Phys.* **1987**, *87*, 2812.

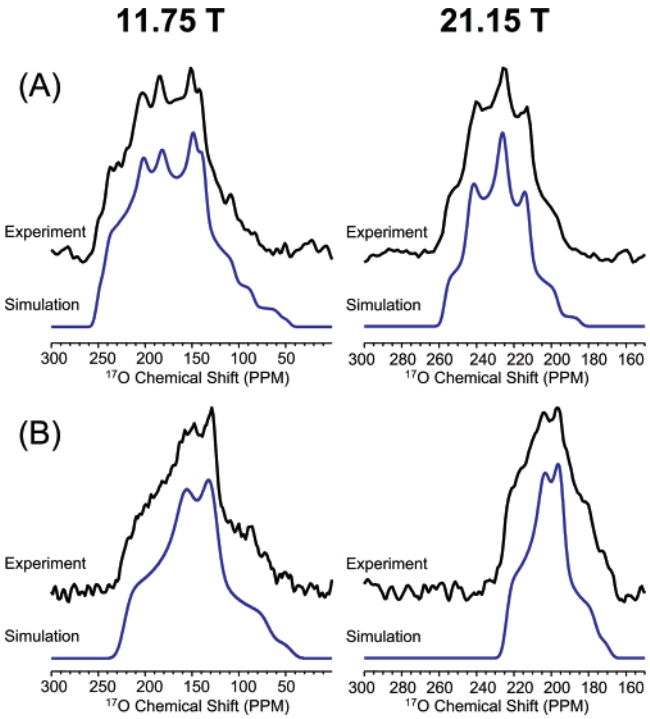

Figure 2. Experimental and simulated ^{17}O MAS NMR spectra for (A) [6-^{17}O]guanosine·2H_2O and (B) [6-^{17}O]guanosine/K^+ gel at 11.75 and 21.15 T. The following experimental parameters were used. (A) 11.75 T, 120-mg sample, 14.5 kHz spinning rate, 22 477 transients, 2-s recycle delay; 21.15 T, 50-mg sample, 18 kHz spinning rate, 5131 transients, 10-s recycle time. (B) 11.75 T, 120-mg sample, 14.5 kHz spinning rate, 36 823 transients, 1-s recycle delay; 21.15 T, 50-mg sample, 20 kHz spinning rate, 2110 transients, 1-s recycle delay.

As shown in Figure 1, the powder XRD data for [6-^{17}O]-guanosine confirm that the solid guanosine sample is indeed in its dihydrate form, **G1**·2H_2O.[55] The powder XRD spectrum for the **G1**/K^+ gel sample exhibits a characteristic peak at $d = 3.31$ Å, which corresponds to the spacing between two adjacent G-quartets. This observation also confirms the formation of stacking G-quartets in the **G1**/K^+ gel sample. As discussed later, this spacing information is further used to build a model for quantum chemical calculations.

Analysis of ^{17}O MAS Spectra. Figure 2 shows the ^{17}O MAS spectra for **G1**·2H_2O obtained at 11.75 and 21.15 T. The observed complex spectral features immediately suggest the presence of multiple oxygen sites. The crystal structure of **G1**·2H_2O indeed indicates that there are two guanosine molecules in the asymmetric unit.[41] We were able to analyze the experimental ^{17}O MAS spectra using a two-site model and simultaneously fit the spectra obtained at two magnetic fields with the same sets of ^{17}O NMR parameters. The resultant ^{17}O quadrupole parameters and isotropic ^{17}O chemical shifts for these two sites are given in Table 1. In principle, ^{17}O multiple-quantum magic-angle spinning (MQMAS) or double-rotation (DOR) spectra can provide independent confirmation for these spectral parameters.[16,56] Unfortunately, as we typically had small quantity (ca. 50 mg) of 10% ^{17}O-enriched [6-^{17}O]guanosine samples, we did not attempt to acquire ^{17}O MQMAS or DOR spectra for these samples. As will be discussed in detail later, we relied on the ^{17}O NMR tensor results from quantum chemical calculations to assign the observed spectral parameters to the two crystallographically distinct sites.

Table 1. Experimental Solid-State ^{17}O NMR Parameters Obtained from Analyses of ^{17}O MAS Spectra at 11.75 and 21.15 T

compound	δ_{iso} (ppm) ±2 ppm	C_Q (MHz) ±0.1 MHz	η_Q ±0.05
[6-^{17}O]guanosine dihydrate			
molecule A	263	7.8	0.44
molecule B	250	7.7	0.55
[6-^{17}O]guanosine/K^+ gel	225	7.2	0.68
triacetyl-[6,^{17}O]guanosine/Sr^{2+} octamer	233	7.0	1.00
triacetyl-[6,^{17}O]guanosine/Ba^{2+} octamer	237	6.9	1.00
triacetyl-[6,^{17}O]guanosine/Pb^{2+} octamer	229	6.4	1.00

Figure 2 also shows the ^{17}O MAS spectra obtained for the **G1**/K^+ gel. In this case, a characteristic NMR line shape arising from second-order quadrupole interaction is observed, indicating that in this system all O6 atoms are equivalent. The most important difference between the carbonyl oxygen atoms in **G1**·2H_2O and **G1**/K^+ gel is the presence of ion−carbonyl interactions in the latter system. As seen from Table 1, the isotropic ^{17}O chemical shift observed for **G1**/K^+ gel is considerably smaller (by 25−30 ppm) than those for **G1**·2H_2O. Similarly, the ion−carbonyl interaction also causes changes in the ^{17}O quadrupole parameters for the O6 atom. In particular, the ^{17}O quadrupole coupling constant is reduced in **G1**/K^+ gel by 0.5 MHz, whereas the asymmetry parameter is increased from $\eta_Q = 0.44$, 0.55 in **G1**·2H_2O to $\eta_Q = 0.68$ in **G1**/K^+ gel. These trends are quite similar to the effects of hydrogen-bonding interactions on ^{17}O NMR parameters observed previously for carbonyl oxygens.[12,17]

Figure 3 shows the ^{17}O MAS spectra for **G2**/M^{+2} octamers (M = Sr, Ba, Pb) obtained at 11.75 and 21.15 T. For these samples, because we had only a very small quantity for each sample (ca. 30−40 mg, 10% ^{17}O), the signal-to-noise ratio in the spectra was generally low, especially for the spectra obtained at the low field, 11.75 T. Nonetheless, these ^{17}O MAS spectra can also be fitted, and the spectral parameters obtained from analyses are also reported in Table 1. Similar to the observations made for **G1**/K^+ gel, the isotropic ^{17}O chemical shifts and the ^{17}O quadrupole parameters observed for **G2**/M^{+2} octamers are quite different from those for G-ribbons. It is interesting to note that, although the isotropic ^{17}O chemical shifts for **G2**/M^{+2} octamers are similar to that observed for **G1**/K^+ gel, the observed ^{17}O quadrupole coupling constants ($C_Q = 6.4-7.0$ MHz) and the asymmetry parameters ($\eta_Q = 1.0$) all suggest an ion−carbonyl interaction present in **G2**/M^{+2} octamers stronger than that in the **G1**/K^+ gel ($C_Q = 7.2$ MHz and $\eta_Q = 0.68$). This effect becomes even more significant considering the fact that each O6 atom in the **G1**/K^+ gel is coordinated to two K^+ ions, whereas in the **G2**/M^{2+} octamers, each O6 atom is coordinated to only one M^{2+} ion. The different trends observed in ^{17}O chemical shifts and ^{17}O quadrupole parameters may be used for probing the mode of ion binding between monovalent and divalent cations and the carbonyl oxygen.

Determination of ^{17}O NMR Tensors. To obtain information about the ^{17}O quadrupole coupling *tensor* and the chemical shift *tensor*, we performed ^{17}O NMR experiments for nonspinning (stationary) samples. Figure 4 shows the stationary spectra for

(55) Sugawara, Y.; Iimura, Y.; Iwasaki, H.; Urabe, H.; Saito, H. *J. Biomol. Struct. Dyn.* **1994**, *11*, 721.
(56) Wong, A.; Howes, A. P.; Pike, K. J.; Lemaitre, V.; Watts, A.; Anupold, T.; Past, J.; Samoson, A.; Dupree, R.; Smith, M. E. *J. Am. Chem. Soc.* **2006**, *128*, 7744.

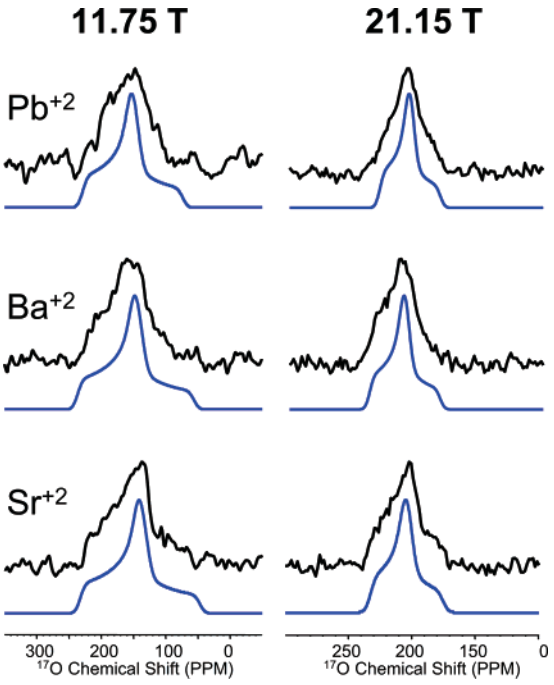

Figure 3. Experimental and simulated ^{17}O MAS NMR spectra for 2′,3′,5′-*O*-triacetyl-[6-^{17}O]guanosine complexes with divalent metal ions at 11.75 and 21.15 T. Each sample was approximately 30−40 mg. Detailed experimental parameters are as follows. Pb^{2+}: 11.75 T, 12.5 kHz spinning rate, 119 577 transients, 2-s recycle delay; 21.15 T, 18 kHz spinning rate, 33 509 transients, 1-s recycle delay. Sr^{2+}: 11.75 T, 21.15 T, 18 kHz spinning rate, 6974 transients, 1-s recycle delay. Ba^{2+}: 11.75 T, 12.5 kHz spinning rate, 37 081 transients, 2-s recycle delay; 21.15 T, 18 kHz spinning rate, 11 025 transients, 1-s recycle delay.

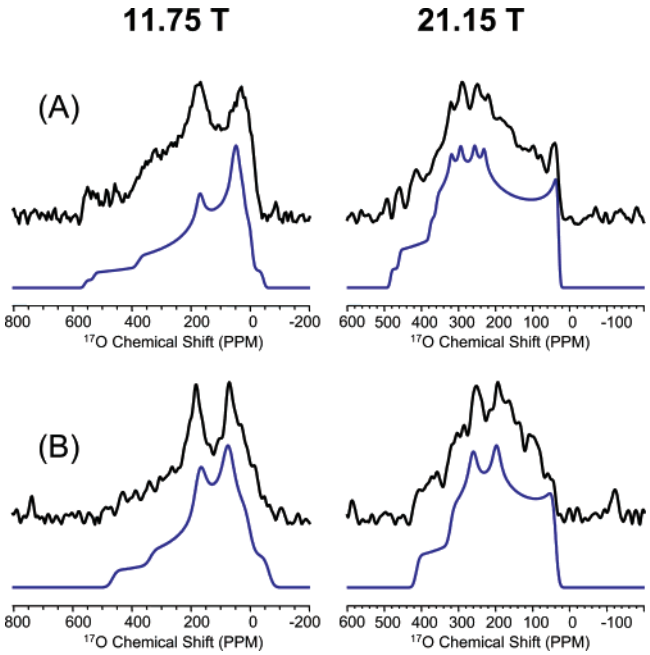

Figure 4. Experimental and simulated ^{17}O NMR spectra for stationary samples of (A) [6-^{17}O]guanosine·$2H_2O$ and (B) [6-^{17}O]guanosine/K^+ gel obtained at 11.75 and 21.15 T. Detailed experimental parameters are as follows. (A) 11.75 T, 120-mg sample, 30 830 transients, 2-s recycle delay; 21.15 T, 50-mg sample, 30 501 transients, 2-s recycle delay. (B) 11.75 T, 50-mg sample, 132 080 transients, 1-s recycle delay; 21.15 T, 50-mg sample, 7719 transients, 1-s recycle delay.

G1·$2H_2O$ and **G1**/K^+ gel obtained at 11.75 and 21.15 T. Because the isotropic chemical shifts and quadrupole parameters have been determined from the aforementioned analyses of ^{17}O MAS spectra, the only remaining variables include two independent chemical shift tensor components and three Euler angles that define the relative orientation between the chemical shift tensor and the quadrupole coupling tensor in the molecular frame of reference. In general, we use the tensor orientations obtained from quantum chemical calculations as a starting point in spectral simulation. Very often, we found that these initial values do not need any further changes. As a result, one only needs to find the values for two independent chemical shift tensor components that would *simultaneously* fit the stationary ^{17}O NMR spectra obtained at two magnetic fields. A more detailed description about spectral analysis for stationary ^{17}O NMR spectra can be found in one of our earlier publications.[12] Results for the ^{17}O NMR tensors in **G1**·$2H_2O$ and **G1**/K^+ gel are summarized in Table 2. It is clear that the observed ^{17}O isotropic chemical shift change in the G-quartet is caused by significant reductions in both δ_{11} and δ_{22} tensor components, whereas δ_{33} appears to be insensitive to the ion−carbonyl interaction. Compared with the strong hydrogen bonding in G-ribbons, the span of the ^{17}O chemical shift tensor for the G-quartet is further reduced by approximately 50 ppm. We found the same relative orientation between the ^{17}O quadrupole coupling tensor and chemical shift tensor in G-ribbons and in G-quartets, which is also confirmed by the quantum chemical calculation as discussed in the next section. The tensor orientations in the molecular frame of reference are depicted in Figure 5.

Calculations of ^{17}O NMR Tensors in G-Ribbons. As mentioned in the previous section, we used the ^{17}O NMR tensor orientations from quantum chemical calculations as initial fitting parameters in our spectral analysis. In this section, we present the details of our model building and quantum chemical calculations for G-ribbons. For **G1**·$2H_2O$, molecular models were constructed from the actual crystal structure for this compound.[41] In the crystal lattice of **G1**·$2H_2O$, guanosine molecules are linked by O6···H−N2 and N7···H−N1 hydrogen bonds, forming G-ribbons of type A as defined in Scheme 2. There are two crystallographically distinct G-ribbons in the crystal lattice running in opposite directions along the crystallographic *b*-axis. Within each G-ribbon, all guanosine molecules are symmetry-related. The main difference between the two G-ribbons in the crystal lattice of **G1**·$2H_2O$ is the strength of hydrogen bonding between guanine bases. Specifically, the O6···H−N2 and N7···H−N1 hydrogen bond lengths are quite different in the two G-ribbons (Molecule A: 2.990 and 2.876 Å; Molecule B: 2.919 and 2.816 Å). Thus, the O6 atom of Molecule B experiences a hydrogen-bonding interaction stronger than that of Molecule A. However, it is also noted that the difference between the two C═O6 bonds is rather small: 1.234 Å (Molecule A) versus 1.238 Å (Molecule B). In both G-ribbons, each O6 atom is also weakly hydrogen bonded to two water molecules of hydration with slightly different O6···O_W distances (Molecule A: 2.930 and 2.938 Å; Molecule B: 2.919 and 3.294 Å). To model the complete hydrogen-bonding environment around the target O6 atom in a G-ribbon, we selected a three-molecule fragment and two water molecules of hydration, as illustrated in Figure 6. The calculated ^{17}O NMR tensors for these G-ribbon models are given in Table 3. It is quite clear that the calculated ^{17}O NMR tensors for the two

Table 2. Solid-State ^{17}O NMR Tensors[a] Obtained from Analyses of ^{17}O MAS and Static Spectra at 11.75 and 21.15 T

compound	δ_{iso} (ppm) ±2 ppm	δ_{11} (ppm) ±5 ppm	δ_{22} (ppm) ±5 ppm	δ_{33} (ppm) ±5 ppm	Ω (ppm)[b] ±10 ppm
[6-^{17}O]guanosine dehydrate					
molecule A	263	460	360	−30	490
molecule B	250	440	340	−30	470
[6-^{17}O]guanosine/K^+ gel	225	400	300	−20	420

[a] The relative orientation between the CS and QC tensors is $\alpha = 0 \pm 10$, $\beta = 90 \pm 2$, $\gamma = 70 \pm 5°$. [b] Span of the chemical shift tensor: $\Omega = \delta_{11} - \delta_{33}$.

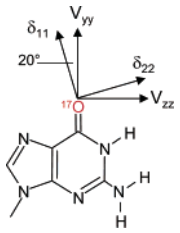

Figure 5. Orientations of the ^{17}O QC and CS tensors in the molecular frame of reference for G-ribbon and G-quartet.

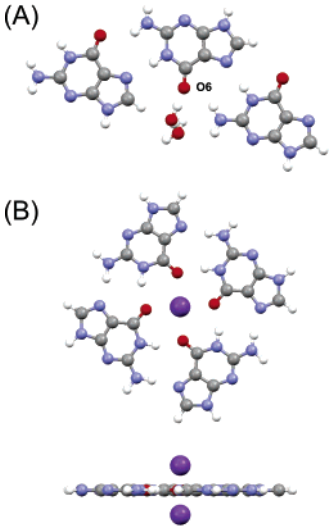

Figure 6. Molecular cluster models for (A) G-ribbon and (B) G-quartet (top and side views) used in quantum chemical calculations.

G-ribbons in **G1**·2H_2O are in reasonable agreement with the experimental ones. The accuracies in both experimental and computational results are sufficiently high to allow an unambiguous assignment of the experimental ^{17}O NMR tensors to the two crystallographically distinct guanosine molecules in **G1**·2H_2O. The observed discrepancies between the two sets of ^{17}O NMR tensors in **G1**·2H_2O reflect essentially the aforementioned difference in hydrogen bonding between guanine bases. As seen in Figure 3, spectral differences on the order of $\Delta\delta_{iso} = 13$ ppm, $\Delta C_Q = 0.1$ MHz, and $\Delta\eta_Q = 0.11$ can be readily detected in the ^{17}O MAS spectra, especially with the utility of a high magnetic field, 21.15 T. This example further illustrates the sensitivity of ^{17}O NMR parameters on hydrogen-bonding interactions. If one examines the individual ^{17}O chemical shift tensor components for Molecules A and B, the subtle difference in hydrogen bonding can cause a change of ca. 20−30 ppm in both δ_{11} and δ_{22} tensor components. The observed trends in $\Delta\delta_{iso}$, ΔC_Q, and $\Delta\eta_Q$ are all in agreement with our previous observations.[12,17] As seen in Table 3, we also computed the ^{17}O NMR tensors for an isolated guanine and for the G-ribbons in the absence of the water molecules of hydration. The calculated

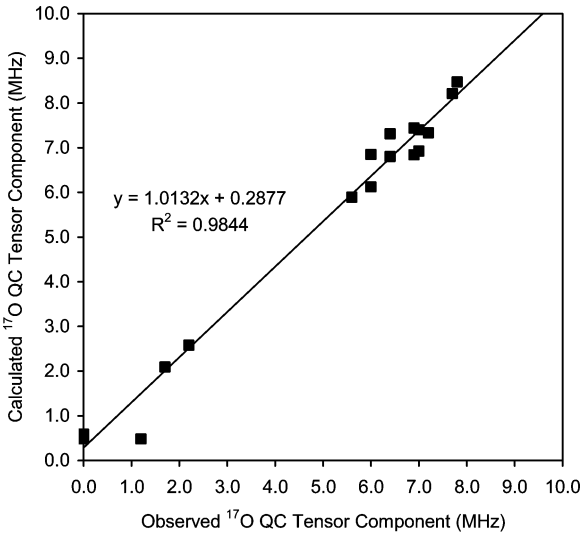

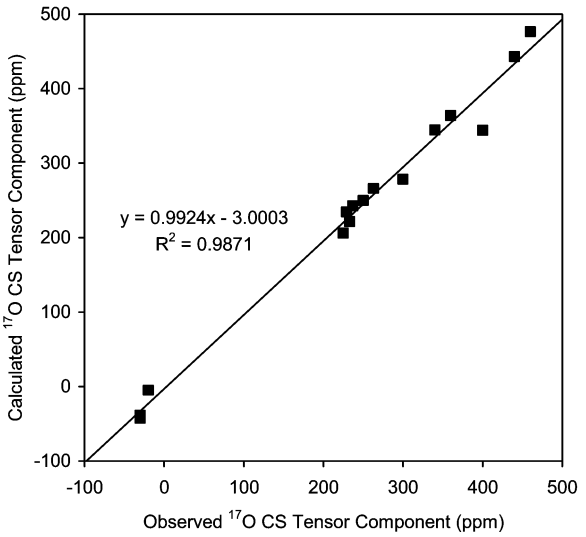

Figure 7. Comparison between computed and observed ^{17}O NMR tensors for G-ribbons and G-quartets. For the QC tensor components, only the absolute values are displayed.

results suggest that the G-ribbon formation alone induces significant changes in the ^{17}O NMR tensors: $\Delta\delta_{iso} \approx 75$ ppm, $\Delta\Omega \approx 110$ ppm, $\Delta C_Q \approx 1$ MHz, and $\Delta\eta_Q \approx 0.12$. The corresponding change in the individual ^{17}O chemical shift tensor components can exceed 100 ppm. The computational results also show that the weak hydrogen-bonding effect from the two water molecules of hydration causes further changes in the ^{17}O chemical shielding tensor and in the ^{17}O quadrupole coupling tensor: 20% in $\Delta\delta_{iso}$, and 3 and 25% in ΔC_Q and $\Delta\eta_Q$, respectively. Therefore, the strong hydrogen bonding in the G-ribbon motif is primarily responsible for the observed ^{17}O NMR tensors. It is important to point out that the hydrogen-

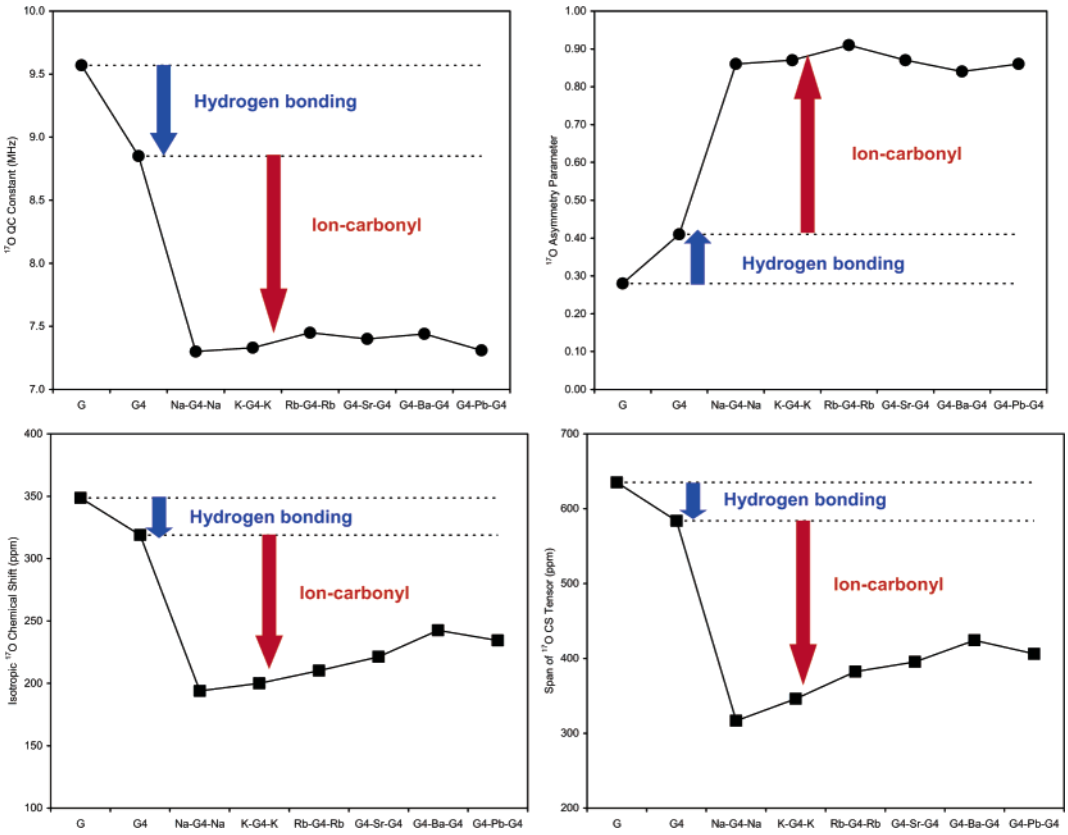

Figure 8. Effects of hydrogen bonding and ion−carbonyl interactions on ^{17}O NMR parameters in G-quartets. Lines connecting the data points are used simply to guide the eyes.

Table 3. Summary of DFT Computational Results for the ^{17}O NMR Tensors at O6 of Guanine in G-Ribbon and G-Quartet Models

system	δ_{iso} (ppm)	δ_{11} (ppm)	δ_{22} (ppm)	δ_{33} (ppm)	Ω (ppm)[b]	C_Q (MHz)	η_Q
guanine	348.6	609.4	461.9	−25.6	635.0	9.57	0.28
G-ribbon (no water)							
molecule A	278.0	503.7	379.3	−49.1	552.8	8.48	0.37
molecule B	273.7	492.4	373.6	−45.0	537.4	8.29	0.43
guanosine dihydrate							
molecule A	265.9	476.4	363.9	−42.5	518.9	8.47	0.39
molecule B	249.8	443.2	344.5	−38.4	481.7	8.21	0.49
empty G_4 (no metal ion)	318.8	561.4	417.3	−22.3	583.7	8.85	0.41
$Na^{+}{-}G_4{-}Na^{+}$	194.0	311.1	276.4	−5.6	316.7	7.30	0.86
$K^{+}{-}G_4{-}K^{+}$	205.8	344.0	278.3	−5.0	349.0	7.33	0.87
$Rb^{+}{-}G_4{-}Rb^{+}$	210.2	369.4	274.0	−12.9	382.2	7.45	0.91
$G_4{-}Na^{+}$ (in-plane binding)	224.9	373.4	316.1	−14.9	388.3	7.62	0.79
$G_4{-}Sr^{+2}{-}G_4$	221.3	378.7	301.6	−16.5	395.2	7.40	0.87
$G_4{-}Ba^{+2}{-}G_4$	242.5	420.1	311.6	−4.1	424.2	7.44	0.84
$G_4{-}Pb^{+2}{-}G_4$	234.4	399.5	310.1	−6.5	406.0	7.31	0.86

bonding interactions observed in G-ribbons are significantly stronger than those present in amides[12] and polypeptides,[27] thus causing much larger changes in ^{17}O NMR tensors.

Calculations of ^{17}O NMR Tensors in G-Quartets. To model the G-quartet structure in **G1**/K^+ gel, we constructed a cluster model consisting of one G-quartet and two K^+ ions (denoted as $K^{+}{-}G_4{-}K^{+}$) as shown in Figure 6. The geometry of the G-quartet is based on that reported by Meyer and co-workers.[57,58] Within the G-quartet, the O6···H−N1 and N7···H−N2 hydrogen bonds are 2.867 and 2.907 Å, respectively. The two central K^+ ions are separated by 3.31 Å, which was determined by powder XRD. The calculated ^{17}O NMR tensors for the $K^{+}{-}G_4{-}K^{+}$ model are also given in Table 3. Also shown in Table 3 are the computed results for $Na^{+}{-}G_4{-}Na^{+}$ and $Rb^{+}{-}G_4{-}Rb^{+}$ models.

For the **G2**/M^{+2} (M = Sr, Ba, Pb) octamers, we constructed a true octamer model consisting of two stacking G-quartets with a 45° twist with each other and one central metal ion (i.e., $G_4{-}M^{+2}{-}G_4$). This model consists of a total of 129 atoms. The M^{+2}···O6 distance in the **G2**/M^{+2} octamers is 2.63 Å, and the diagonal O6···O6 distance within the G-quartet is 4.46 Å. These are comparable to the X-ray crystal structural data reported by Davis and co-workers for similar lipophilic G-quartets containing Sr^{2+}, Ba^{2+}, and Pb^{2+} ions.[59−61] The calculated ^{17}O NMR tensors for these octamers are also shown in Table 3. In general,

(57) Meyer, M.; Steinke, T.; Brandl, M.; Suhnel, J. *J. Comput. Chem.* **2001**, *22*, 109.
(58) Meyer, M.; Hocquet, A.; Suhnel, J. *J. Comput. Chem.* **2005**, *26*, 352.

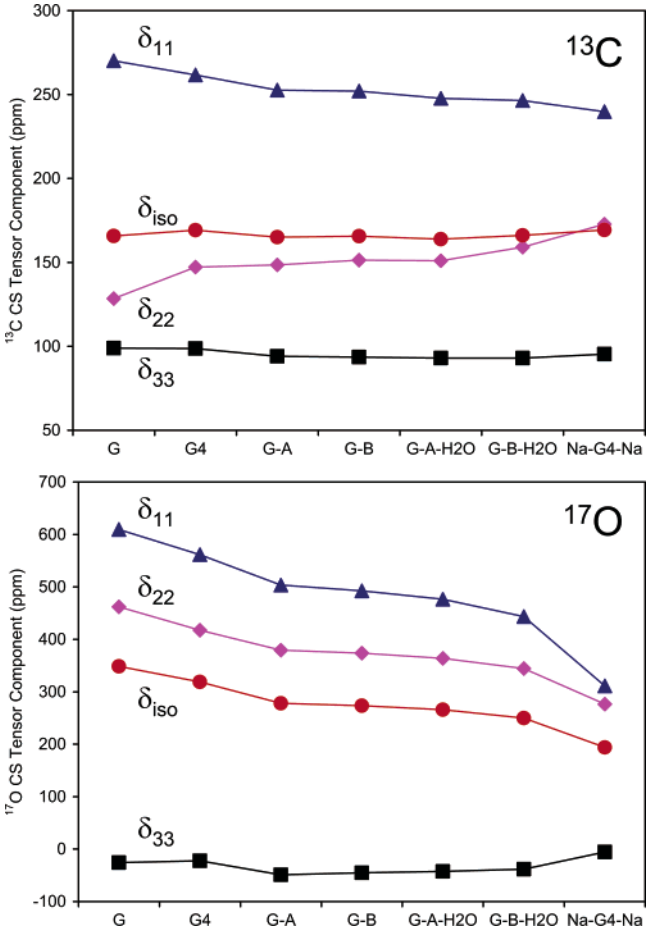

Figure 9. Dependence of ^{13}C (top) and ^{17}O (bottom) CS tensors on the presence of hydrogen bonding and ion−carbonyl interactions.

as illustrated in Figure 7, the calculated ^{17}O chemical shift and quadrupole coupling tensors for G-ribbons and G-quartets are in reasonable agreement with the experimental results. All the observed trends in ^{17}O NMR tensors were reproduced by the DFT calculations.

Separation of Hydrogen Bonding and Ion−Carbonyl Interactions. Another objective of performing quantum chemical calculations is to be able to separate the effects of hydrogen bonding and ion−carbonyl interactions. To this end, we calculated the ^{17}O NMR tensors for an empty G-quartet model (Table 3). Comparison of the ^{17}O NMR tensors calculated for these different models allows the separation of the effect from ion−carbonyl interactions from hydrogen-bonding interactions. As shown in Figure 8, the hydrogen bonding in the G-quartet is responsible for $\Delta C_Q = 0.7$ MHz, $\Delta\eta_Q = 0.13$, $\Delta\delta_{iso} = 30$ ppm, and $\Delta\Omega = 52$ ppm. Interestingly, these changes are not as large as those caused by the formation of a G-ribbon. On the other hand, the ion−carbonyl interaction in the G-quartet causes further changes of the ^{17}O NMR parameters: $\Delta C_Q > 1.4$ MHz, $\Delta\eta_Q > 0.45$, $\Delta\delta_{iso} > 100$ ppm, and $\Delta\Omega > 180$ ppm. Apparently, the ion−carbonyl interaction causes significantly larger changes in the ^{17}O NMR parameters than does the hydrogen-bonding interaction. It should be mentioned that, although the computed results are similar for all the G-quartet models shown in Figure 8, the ion−carbonyl interaction from a divalent cation is clearly much greater than that from a single monovalent cation; the apparently similar results are simply due to the different binding modes between divalent and monovalent cations: O6···M^{2+} versus M^+···O6···M^+. This conclusion is in agreement with that made by Chekmenev et al.[27] regarding the effect of Li^+ and Ca^{2+} on the ^{17}O NMR tensors of a peptide carbonyl oxygen.

For completeness, we also computed the ^{17}O NMR tensors for a G-quartet containing a Na^+ ion in an in-plane binding mode. This type of ion binding to a G-quartet has been observed only for Na^+ in two G-quadruplex DNA oligomers.[62,63] Other alkali metal ions such as K^+ and Rb^+ are too large to fit into the center of a G-quartet. The computed ^{17}O NMR tensors for the in-plane binding mode exhibit $\Delta\delta_{iso} = 30$ ppm, $\Delta C_Q = 0.32$ MHz, and $\Delta\eta_Q = -0.07$, compared to those for the cavity binding mode, $G_4-Na^+-G_4$. Such changes in ^{17}O NMR parameters suggest that the O6 atom experiences overall a weaker ion−carbonyl interaction when a single Na^+ ion is located in the G-quartet plane than when two Na^+ ions are out of the plane. This is another example where a single strong Na^+···O6 interaction ($R_{Na\cdots O6} = 2.285$ Å) in G_4-Na^+ is overtaken by the sum of two weak Na^+···O6 interactions ($R_{Na\cdots O6} = 2.818$ Å) in $Na^+-G_4-Na^+$. These spectral differences may be used to distinguish these two modes of Na^+ binding to a G-quartet. In this regard, we showed recently that ^{23}Na NMR parameters for Na^+ ions are also sensitive to the mode of Na^+ binding and that $\delta_{iso}(^{23}Na)$ is perhaps a better probe for the detection of different Na^+ binding modes in G-quartets.[64] It is certainly an ideal situation if a particular ion−carbonyl interaction can be studied from both sides. That is, simultaneous detection of ^{17}O NMR signals for the carbonyl group and metal NMR for the ion would yield most reliable information about the ion−carbonyl interaction.

Comparison between ^{17}O and ^{13}C Chemical Shift Tensors. Because both ^{17}O and ^{13}C chemical shift tensors were generated in the same set of quantum chemical calculations, it is worth examining how the ^{13}C chemical shifts of the carbonyl carbon respond to both hydrogen bonding and ion−carbonyl interactions in G-ribbons and G-quartets. As shown in Figure 9, as the strength of hydrogen bonding and ion−carbonyl interactions increases, two of the ^{13}C CS tensor components, δ_{11} and δ_{22}, change in opposite directions by approximately the same amounts. Meanwhile the ^{13}C CS component δ_{33} is insensitive to these interactions. As a result, the isotropic ^{13}C chemical shift is also rather insensitive to the presence of hydrogen bonding and ion−carbonyl interactions, simply due to a partial cancellation between δ_{11} and δ_{22} components. This trend has also been observed for the backbone carbonyl carbon in peptides and proteins.[65,66] In contrast, the isotropic ^{17}O chemical shift is much more sensitive to hydrogen bonding and ion−carbonyl interactions, because δ_{11} and δ_{22} components change in the same direction, thus enhancing the effect. These calculated results

(59) Shi, X. D.; Fettinger, J. C.; Davis, J. T. *J. Am. Chem. Soc.* **2001**, *123*, 6738.
(60) Kotch, F. W.; Fettinger, J. C.; Davis, J. T. *Org. Lett.* **2000**, *2*, 3277.
(61) Shi, X.; Fettinger, J. C.; Davis, J. T. *Angew. Chem., Int. Ed.* **2001**, *40*, 2827.
(62) Laughlan, G.; Murchie, A. I. H.; Norman, D. G.; Moore, M. H.; Moody, P. C. E.; Lilley, D. M. J.; Luisi, B. *Science* **1994**, *265*, 520.
(63) Horvath, M. P.; Schultz, S. C. *J. Mol. Biol.* **2001**, *310*, 367.
(64) Ida, R.; Kwan, I. C. M.; Wu, G. *Chem. Commun.*, published online Nov 15, 2006 http://dx.doi.org/10.1039/b613105k.
(65) de Dios, A. C.; Oldfield, E. *J. Am. Chem. Soc.* **1994**, *116*, 11485.
(66) Wei, Y. F.; Lee, D.-K.; Ramamoorthy, A. *J. Am. Chem. Soc.* **2001**, *123*, 6118.

demonstrate that ^{17}O NMR is a much better probe than ^{13}C NMR for studying a carbonyl group (C═O) involved in either hydrogen bonding or ion−carbonyl interactions.

4. Conclusion

In this study, we have determined the ^{17}O quadrupole coupling tensor and chemical shift tensor for the carbonyl oxygen O6 of guanine in several [6-^{17}O]guanosine derivatives that form either G-ribbons or G-quartets. This work represents the first experimental characterization of ^{17}O NMR tensors in these structures. The observed ^{17}O quadrupole coupling and chemical shift tensors exhibit remarkable sensitivity to the presence of both hydrogen bonding and ion−carbonyl interactions. We have found that the effect from ion−carbonyl interactions is significantly greater than that from hydrogen-bonding interactions. Our computational results illustrate that ^{17}O NMR exhibits a much greater sensitivity to the presence of hydrogen bonding and ion−carbonyl interactions than does ^{13}C NMR for the C6═O6 carbonyl group in guanine. This conclusion is also generally true for other carbonyl groups such as the peptide carbonyl group. Our results have not only confirmed the sensitivity of ^{17}O NMR tensors to hydrogen bonding, but also established a new basis for solid-state ^{17}O NMR studies of ion binding. The results present in this work, together with the recent findings of Chekmenev et al.,[27,28] have clearly demonstrated the potential of solid-state ^{17}O NMR for biological systems. It is also important to keep in mind that the experimental data presented in this study should be considered as benchmarks for ion−carbonyl interactions in G-quartets. In real biological systems, ion-binding phenomena are often associated with a dynamic process. Under such circumstances, the observable effect may be complicated by either short residence time or partial occupancy. Nevertheless, the solid-state ^{17}O NMR approach demonstrated here promises to offer a new angle into the study of this fundamental molecular interaction. We are currently exploring the possibility of introducing ^{17}O labels into G-quadruplex DNA.

Acknowledgment. This work was supported by the Natural Sciences and Engineering Research Council (NSERC) of Canada. Quantum chemical calculations were performed at the High Performance Computing Virtual Laboratory (HPCVL) at Queen's University. Access to the 900 MHz NMR spectrometer was provided by the National Ultrahigh Field NMR Facility for Solids (Ottawa, Canada), a national research facility funded by the Canada Foundation for Innovation, the Ontario Innovation Trust, Recherche Québec, the National Research Council Canada, and Bruker BioSpin and managed by the University of Ottawa (http://www.nmr900.ca). We thank Dr. Victor Terskikh for technical assistance.

Supporting Information Available: Complete citation for ref 49. 1D ^{1}H and 2D NOESY NMR spectra for **G2**/M^{2+} octamers in $CDCl_3$. Atomic coordinates (in PDB format) of the G-ribbon and G-quartet models. This material is available free of charge via the Internet at http://pubs.acs.org.

JA067991M